TURBULENT VISCOSITY FOR THE ANALYSIS OF AN INCOMPRESSIBLE BOUNDARY LAYER ON A ROUGH SURFACE

G. F. Sivykh

UDC 532.526.4

There exist two approaches to the determination of the turbulent boundary-layer characteristics, integral and differential (finite-difference methods). The former approach is related to utilization of integral relations when the boundary-layer equations are satisfied only in the mean in its thickness, and permit the computation of just the integral characteristics such as the friction coefficient, the thickness of the loss of momentum, etc. Examples of using integral methods for boundary-layer analysis on rough surfaces can be found in [1, 2], for example.

Differential methods that contain direct assumptions about the Reynolds stresses at a point and are associated with the solution of the fundamental partial differential equations of the conservation laws, permit more enhanced information to be obtained. Differential methods are separated in [3] into models closed by using the mean velocity field, and models in which the field of average turbulence characteristics are used. In the former case sufficiently simple models based on the turbulent viscosity (or the mixing path) concept [4] are used to obtain the magnitudes of the turbulent tangential stresses and the mean velocity field, and successfully in many cases.

In this paper a turbulent viscosity model is proposed for the analysis of a two-dimensional incompressible boundary layer with a pressure gradient on a permeable rough surface.

1. In formulating problems by using turbulent viscosity, the representation of a two-layer boundary layer with different viscosity variation laws in the inner (near-wall) and outer regions is ordinarily used. It is known (see [5], for example) that the large-scale motion responsible for the characteristics of the external zone depends weakly on the wall state. Consequently, it is natural to use methods developed for the analysis of the boundary layer on a smooth surface [3, 4] in the outer domain. In this paper, the mixing path model

$$\frac{\mu_t}{\mu} = l^{+2}\left|\frac{\partial u^+}{\partial y^+}\right|, \quad u^+ = \frac{u}{u_*}, \quad y^+ = \frac{\rho u_* y}{\mu}, \quad l^+ = \frac{\rho u_* l}{\mu}, \tag{1.1}$$

was used in performing the computations, where y is the coordinate normal to the surface; u, longitudinal velocity component; ρ, density; μ and μ_t, the molecular and turbulent viscosities; $u_* = (\tau_w/\rho)^{1/2}$, dynamical velocity; τ, shear stress; and the subscript w denotes parameters at the wall. The mixing path length l in the external domain is assumed proportional to the boundary-layer thickness $l = 0.09\delta$.

As is known, the possibility of utilizing a local representation of the effects of turbulent exchange in the external domain by using (1.1) is limited to the case of almost "equilibrium" flows. In analyzing "strongly nonequilibrium" flows, preference should be for models of average turbulence characteristics transfer [3]. In contrast to the external domain, the fine-scale turbulence of the near-wall zone possesses a "short memory" since perturbation damping occurs here at short ranges. This circumstance permits successful utilization of the local approach conception near the wall and obtaining an algebraic expression for the turbulent viscosity. Let us note that because of its local nature it can also be utilized as a boundary condition for the equations of turbulent characteristics transport in the analysis of "strongly nonequilibrium" flows.

We use the equation of motion which has the following form:

$$\left(1 + \frac{\mu_t}{\mu}\right)\frac{du^+}{dy^+} = \tau^+, \quad \tau^+ \equiv \frac{\tau}{\tau_w} = 1 + p^+ y^+ + v_w^+ u^+, \quad p^+ = \frac{\mu}{\rho^2 u_*^3}\frac{dp}{dx}, \quad v_w^+ = \frac{v_w}{u_*}, \tag{1.2}$$

Novosibirsk. Translated from Zhurnal Prikladnoi Mekhaniki i Tekhnicheskoi Fiziki, No. 2, pp. 65-73, March-April, 1984. Original article submitted January 28, 1983.

 0021-8944/84/2502-0226$08.50

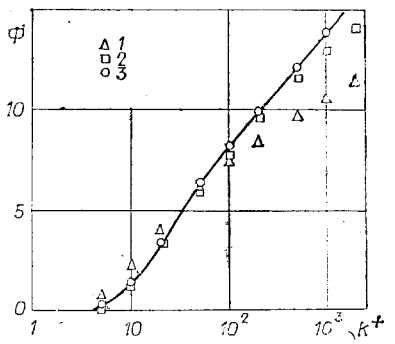

Fig. 1

near the wall where convection in the flow direction can be neglected, where p is the pressure and v is the transverse velocity component. Experimental results obtained for smooth and rough surfaces (see [5], for instance) show that the relationship (1.2) for τ^+ is satisfied with a high degree of accuracy for the whole internal layer. In that case, the correct expression for μ_t should result in agreement between the velocity profile obtained upon integration of (1.2) and the profile obtained on the basis of test data. For instance, when $1 + v^+_w u^+ >> p^+ y^+$, the velocity distribution at sufficient remoteness from the wall roughness can be represented in the form [2, 6]

$$\frac{2}{v^+_w}\left(\sqrt{1 + v^+_w u^+} - 1\right) = \frac{1}{\varkappa} \ln y^+ + B - \Phi\,(k^+, \sigma_1, \sigma_2, \ldots). \tag{1.3}$$

On an impermeable surface $v^+_w = 0$ and the left side of (1.3) equals u^+. Here $\varkappa$ is the Karman turbulence parameter, k is the height of the roughness elements ($k^+ = \rho u_* k/\mu$), and B is the parameter governing the location of the logarithmic section of the profile on a smooth wall, $\Phi(k^+, \sigma_1, \sigma_2, \ldots)$ is the dynamical roughness function representing a shift in the velocity profile because of the influence of roughness, σ_1, σ_2, ... are parameters characterizing the shape of the roughness elements and their distribution over the surface. An approximation of the experimental data obtained by Nikuradze for sandy roughness is shown by the solid curve in Fig. 1. For certain other modes of homogeneous roughness, the set of parameters σ_1, σ_2, ... is successfully reduced in its developed streamline regime [when the dependence $\Phi(k^+, \sigma_1, \sigma_2, \ldots) = \ln (k^+)/\varkappa + R(\sigma_1, \sigma_2, \ldots)$ is correct] to a single distribution density parameter for the elements on the surface λ and a single correlation dependence $R(\lambda)$ is obtained. Let us note an important property of roughness function: Its value in the developed regime is explicitly independent of the mass transfer on the surface, the pressure gradient, the transverse surface curvature, etc. [2, 6].

In [7], devoted to the investigation of the flow in the inner domain, utilization of (1.1) is proposed for the turbulent viscosity in this zone, where the mixing path distribution is given in the form

$$l^+ = \varkappa y^+ [1 - \exp(-y^+/A^+) + \exp(-60 y^+/A^+ k^+)], \tag{1.4}$$

where A^+ is the velocity fluctuation damping parameter near the wall. On a hydraulically smooth surface $k^+ \to 0$ and the second exponential term is negligible. Utilization of (1.4) for a smooth surface (see [4], for example) is in good agreement with known experimental data. However, a numerical analysis of the velocity profiles on a rough surface, executed by using this representation, will yield an unsatisfactory correspondence between the computation (points 1 in Fig. 1) and the experimental dependence $\Phi(k^+)$.

Utilization of the formula obtained in [8] to this same end improves this correspondence substantially (points 2) but even here a tendency to deviation is observed as k^+ grows. Moreover, the applicability of the expression from [8] is limited to the case of roughness that can be reduced to equivalent sandy roughness which is, as a rule, impossible for the transition mode of the flow around its elements.

Let us obtain an expression for turbulent viscosity by comparing the experimentally established velocity profile to the result of integrating (1.2). We note first that the distribution μ_t will be given by the formula $\mu_t/\mu \approx \varkappa y^+ \sqrt{\tau^+}$ at sufficient remoteness from the smooth wall. We take account of additional vortex formation caused by the roughness elements in an additive manner

$$\mu_t/\mu = (\varkappa y^+ + f(k^+, \sigma_1, \sigma_2, \ldots))\sqrt{\tau^+}. \quad (1.5)$$

An analogous approach to modeling μ_t was used in [9], where gradient-free flow around an impermeable plate was considered. In the general case of the combined action of mass transfer and a pressure gradient, the variables in (1.2) do not separate; consequently, we examine their influence separately. For instance, let $1 + v^+_w u^+ >> p^+ y^+$. Then, by substituting (1.5) into (1.2) and noting that a relationship $1 + (\varkappa y^+ + f)\sqrt{\tau^+} \simeq (1 + \varkappa y^+ + f)\sqrt{\tau^+}$ is valid over the whole thickness of the near-wall domain, we will have, after integration,

$$\frac{2}{v_w^+}\left(\sqrt{1 + v_w^+ u^+} - 1\right) = \frac{1}{\varkappa} \ln \frac{1 + \varkappa y^+ + f}{1 + f}. \quad (1.6)$$

Comparing (1.3) and (1.6) in the domain of validity of the logarithmic velocity distribution (where $\varkappa y^+ >> 1 + f$), we obtain the desired expression for the term modeling the vortex formation on a rough surface

$$f(k^+, \sigma_1, \sigma_2, \ldots) = \frac{\varkappa}{\exp\{\varkappa[B - \Phi(k^+, \sigma_1, \sigma_2, \ldots)]\}} - 1. \quad (1.7)$$

Performing analogous reasoning for a boundary layer with a pressure gradient without mass transfer ($v_w = 0$), we can obtain that additional vortex formation is given by the very same dependence in this case. It is then natural to assume that (1.7) is also valid in the general case of the combined influence of mass transfer of a pressure gradient. The satisfactory agreement between the results of a computation presented in Sec. 3 and experimental data confirms the legitimacy of this assumption.

By using (1.7), the value of the boundary of the developed roughness regime k^+_r that is important for practical applications can be obtained. Indeed, the complete degeneration of the viscous sublayer and its associated effects of the appearance of molecular transfer corresponds to the time of the onset of the developed roughness regime. The same situation is felt at sufficiently long ranges from a smooth wall where $\mu_t/\mu \simeq \varkappa y^+\sqrt{\tau^+}$. Hence, it is clear that $f = 0$ at the boundary of the developed roughness regime, and

$$k_r^+(\sigma_1, \sigma_2, \ldots) = \exp\{\varkappa[B - R(\sigma_1, \sigma_2, \ldots)]\}/\varkappa. \quad (1.8)$$

The expression obtained from k^+_r is in good agreement with the known Nikuradze experimental data for sandy roughness and the Hamm data for baffles (data are presented in [1]). For smaller values $k^+ < k^+_r$ (transition roughness regime) we have $f < 0$, whereupon the residual damping influence of the viscosity is taken into account.

Let us note that the velocity distribution obtained by using (1.5) and (1.7) (the points 3 in Fig. 1) is in good agreement with the corresponding experimental Nikuradze results.

2. In order to verify the validity of the proposed turbulent viscosity model, the results of a finite-difference computation of turbulent boundary-layer characteristics were compared with a number of known experimental data. Taken as the basis of the calculational algorithm was the Patankar–Spalding procedure [4] developed to analyze the boundary layers on a smooth wall. Changes needed to take account of roughness related to the flow zone adjoining the wall were the following. The equations describing the flow in this zone have the following form in the uniform boundary-layer approximation:

$$\frac{d\omega}{dy^+} = \frac{\mu u^+}{\psi_e - \psi_w}, \quad \frac{du^+}{dy^+} = \frac{\tau^+}{1 + \mu_t/\mu}, \quad (2.1)$$

where μ_t/μ is computed by using (1.1) and (1.4) in the case of a smooth surface (when $k^+ \to 0$) and (1.5) and (1.7) in the case of a rough wall; $\omega = (\psi - \psi_w)/(\psi_e - \psi_w)$ is a dimensionless stream function used in [4] as a coordinate normal to the surface, and e is the subscript for the external boundary-layer boundary.

The system of ordinary differential equations (2.1) for the abutting zone was solved by the Runge–Kutta method in combination with finite-difference equations approximating the conservation equation in the remaining portion of the boundary layer. The solutions were merged in the middle of the ω interval closest to the wall. The values of the coordinate y^+_i and the velocity u^+_i corresponding to this point ω_i, were determined during integration of system (2.1).

The difference equations for $\omega_i \leq \omega \leq 1$ were solved by the factorization method across the boundary layer [4]. The turbulent viscosity distribution needed to evaluate the factori-

zation coefficients was computed by the formulas presented in Sec. 1, and in conformity with the two-layer boundary-layer scheme assumed.

In addition to the boundary conditions on the wall and the external boundary-layer boundary, the profiles of all the variables in the initial section must be known in order to solve the system of boundary-layer equations of parabolic type. However, only integral characteristics are presented in the initial section in the majority of cases: the friction coefficient c_f and the thickness of the loss of momentum θ. In such cases, the velocity profile given by the formula

$$\frac{2\varkappa}{v_w^+}\left(\sqrt{1+v_w^+u^+}-1\right)=\ln\frac{1+\varkappa y^++f}{1+f}+g\left(\Pi,\frac{y}{\delta}\right). \tag{2.2}$$

was taken as the initial profile.

In contrast to (1.6), which is valid in the near-wall domain, the wake function $g(\Pi, y/\delta)$ representing the deviation of the velocity profile in the external boundary-layer domain from the logarithmic law is appended here. It is shown in [10] that the wake parameter Π and the wake function are explicitly independent of the mass transfer on a streamlined surface; the conservativity of the wake function relative to the surface roughness is proved in [6]. A convenient and sufficiently exact expression for $g(\Pi, y/\delta)$, assuring a good description of the velocity profile in a broad range of pressure gradients and Reynolds numbers, is proposed in [11]:

$$g(\Pi, y/\delta) = (1 + 6\Pi)(y/\delta)^2 - (1 + 4\Pi)(y/\delta)^3. \tag{2.3}$$

Using (2.2) and (2.3), we obtain relations to determine the parameter Π and the boundary-layer thickness δ for given values of $u^+_e = (2/c_f)^{1/2}$ and θ:

$$\frac{\theta}{\delta}=\left(\frac{c_f}{2}+j\right)^{1/2}(I_1+jI_3)-\left(\frac{c_f}{2}+j\right)I_2-\frac{j}{4}(I_2+jI_4), \tag{2.4}$$

$$\frac{2\varkappa}{v_w^+}\left[(1+v_w^+u_e^+)^{1/2}-1\right]=\ln\left(\frac{1}{\varepsilon}+\frac{1}{\varepsilon}\right)+2\Pi.$$

Here

$$j = v_w/u_e,\quad \varepsilon = (1 + f)/\varkappa\delta^+,$$
$$I_1 = \varkappa^{-1}(\Pi + 0.917 - E_1 + \varepsilon),$$
$$I_2 = \varkappa^{-2}[1{,}486\Pi^2 + (3.043 - 4E_1 + 5{,}33\varepsilon)\Pi + 1.912 + E_2$$
$$I_3 = \varkappa^{-3}[1.229\Pi^3 + (4.048 - 6E_1 + 9{,}13\varepsilon)\Pi^2 + (5{,}37 + 3E_2 + 2{,}17\varepsilon],$$
$$+ 8{,}23\varepsilon)\Pi + 2.943 - E_3/2 + 3{,}26\varepsilon],$$
$$I_4 = \varkappa^{-4}[1.068\Pi^4 + (4.937 - 8E_1 + 13{,}23\varepsilon)\Pi^3 + (10{,}216 + 6E_2 +$$
$$+ 19.1\varepsilon)\Pi^2 + (11.484 - 2E_3 + 15.46\varepsilon)\Pi + 5{,}952 + E_4/4 + 6.38\varepsilon].$$

The parameters E_i ($i = 1, \ldots, 4$) are evaluated from the recursion formula $E_i = -\varepsilon(\ln\varepsilon)^i - iE_{i-1}$, where $E_0 = -\varepsilon$. A formula similar to (2.4) was obtained in [10] for the flow around a smooth surface (when ε, $E_i \to 0$). However, the coefficient $1/4$ is erroneously committed there in front of the last term in the right side of the expression for θ/δ.

The usual conditions at the wall and the external boundary-layer boundary were utilized as boundary conditions

$$y = 0,\ u = 0,\ v = v_w;\quad y = \delta,\ u = u_e(x).$$

As already noted in Sec. 1, the expression $\Phi = (\ln k^+)/\varkappa + R$ is valid for the roughness function in the developed regime ($k^+ \geqslant k^+_r$). The correlation dependence $R(\lambda)$ can be found in [1] for certain roughness element shapes; in a number of other cases the value of the equivalent sandy roughness is known for which $R \approx -3$ [12]. In the transition roughness regime ($k^+_s \leq k^+ \leq k^+_r$) the following approximate formula is sufficiently exact:

$$\Phi=\left(\frac{1}{\varkappa}\ln k^+ + R\right)\sin\left(\frac{\pi}{2}\frac{\ln k^+ - \ln k_s^+}{\ln k_r^+ - \ln k_s^+}\right),$$

where k^+_s is the boundary of the hydraulically smooth streamline regime (for the Nikuradze sandy roughness $k^+_s \approx 5$). It should be expected that the value of k^+_s would increase as the degree of homogeneity of the roughness elements increases.

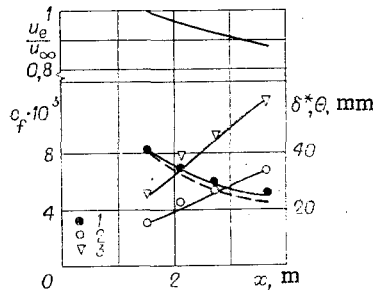

Fig. 2

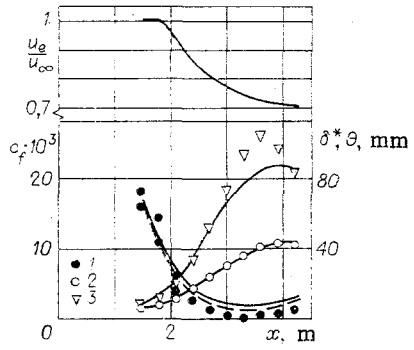

Fig. 3

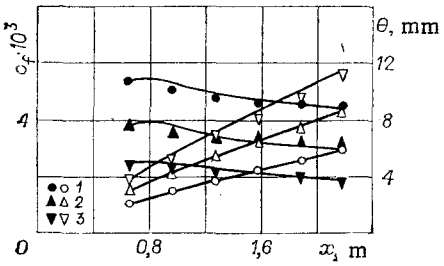

Fig. 4

3. The results of a computation were compared with classical experimental data obtained by Dhavan, Shultz–Grunow, and Kampff on a smooth plate in a broad range of Reynolds numbers $Re_x = 10^5$–10^9 (data presented in [13]) in order to verify the algorithm. For the computation the values of the turbulence parameters were selected equal to $\varkappa = 0.41$ and $A^+ = 26$. The computational mesh was constructed in such a manner that the value of the coordinate y^+_i in the middle of the ω interval closest to the wall would not emerge outside the boundary of the range $y^+_i = 2$-5. The agreement turned out to be quite good (the deviation for c_f did not exceed ±4%); consequently, the values mentioned were used in all the subsequent boundary-layer computations on a rough surface.

The exception was the value of the parameter $\varkappa$ in the gradient flow computation. It turns out that utilization of the same value $\varkappa = 0.41$, as in gradient-free flows, results in a systematic exaggeration of the friction coefficient c_f, as compared with the experimental data, for flow with negative pressure gradient and a reduction in c_f for flows with positive pressure gradient. Results obtained in [14] by processing velocity profiles measured on smooth surfaces in a number of papers also yield a deduction about the dependence of the parameter κ on the longitudinal pressure gradient. On the basis of experimental data presented at the Stanford conference (1968), the following dependence is proposed in [15]:

$$\varkappa = 0.41 + 0.182[1 - \exp(-0.32\beta)], \quad \beta = -0.5\text{–}5, \tag{3.1}$$

where $\beta = \delta^*/\tau_w \cdot dp/dx$ is the Clauser equilibrium parameter and δ^* is the displacement thickness. According to [15], such a correction permits a substantial rise in the accuracy of determining c_f for equilibrium boundary layers (by 30-40% for $\beta \simeq 5$). Because of the above, the value of κ was computed by using (3.1), where β was evaluated for the appropriate state of the surface. In the case of nonequilibrium flows, taking account of the prehistory of the pressure gradient was performed by using a simple relaxation model to compute the effective value of β [16].

By using the turbulent viscosity model developed above, satisfactory agreement was obtained between the results of a computation and all the experimental data for impermeable surfaces available in [1, 8]. Let us present two typical graphs.

Represented in Fig. 2 is a comparison with results of measuring c_f, θ, and δ^* (points 1-3, respectively) in a boundary layer ($u_\infty = 34.45$ m/sec) on a surface covered by two-dimensional roughness elements: Square elements with side k = 3.175 mm were arranged across the flow with a period (density) $\lambda = 4$ [6]. The dashed line here represents results of computing the friction coefficient c_f obtained for $\kappa = 0.41$. As should have been expected, the influence of a change in κ on the integral thicknesses θ and δ^* turned out to be weak; consequently, here and below only results are presented for their computation that correspond to the value $\varkappa(\beta)$ calculated according to (3.1).

Scottron and Power (see [1]) investigated the influence of the pressure gradient on the boundary-layer characteristics near a rough surface formed by using a mesh of square cells (k = 5.34 mm, $\lambda = 3.7$, $u_\infty = 29.9$ m/sec). Represented in Fig. 3 is a comparison with a computation for the case of the strongest unfavorable pressure gradient. As before, points 1-3 denote c_f, θ, δ^* and the dashes a computation of c_f with $\varkappa = 0.41$. Compared with the remaining cases, the agreement here turns out to be not so satisfactory. This can be explained both by the pressure gradient being close to the separation value, and by the three-dimensional nature of the flow near the wall. Both these reasons impose constraints on the possibility of utilizing the two-dimensional boundary-layer model.

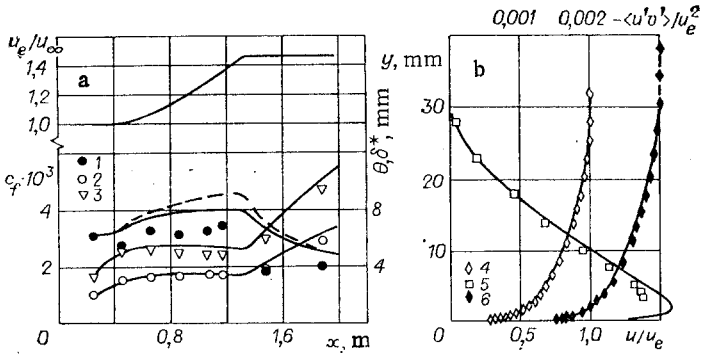

Fig. 5

Before presenting the comparison for permeable surfaces, let us make two remarks relative to the combined influence of mass transfer and the pressure gradient on the parameters used in the computation. The former concerns the parameter B in the near-wall velocity profile (1.3). The influence of blowing on the quantity B in a gradient-free flow is investigated in [17]. Taking into account that the pressure gradient has no influence on B in practice, this dependence can be written in the form

$$B = 2\left(\sqrt{1 + 11v_w^+} - 1\right)/v_w^+ - 6.$$

It is interesting to note that an increase in the blowing parameter v^+_w will result in a diminution of B and a diminution of k^+_r in conformity with (1.8). This deduction about the broadening the zone of the developed roughness regime is in agreement with the experimental observations [5] about the appearance of additional properties inherent to the flow around a rough surface, on a wall with blowing. According to [5], the appearance of these properties is associated with the formation of a decelerating flux of the pressure field around each jet blown in from the surface.

The second remark concerns the utilization of (3.1). It is proved experimentally that (see [5], for example) the mass transfer on the surface does not influence the magnitude of the parameter $\varkappa$. Taking this into account, as well as the fact that the dependence (3.1) is proposed for the boundary layer on a surface without mass transfer, we shall use (3.1) under the condition of replacing the value τ_w by its analog τ_{wo} on an impermeable wall. In a first approximation, we use $\tau_{wo} = \tau_w/[\ln(1 + b)/b]^{0.7}$ for this relationship, where $b = 2j/c_f$ [18]. Then we will have the following modified expression for the equilibrium parameter

$$\beta = \frac{\delta^*}{\tau_w}\left[\frac{\ln(1+b)}{b}\right]^{0,7}\frac{dp}{dx}. \qquad (3.2)$$

Represented in Figs. 4 and 5 is a comparison between a computation and experimental data obtained in [5, 19], respectively. The flow around a porous plate covered compactly by homogeneous spherical roughness elements with radius r = 0.635 mm was investigated in these papers. The nature of the roughness elements does not permit determination of the roughness density λ and use of the correlation dependence [1]. Hence, the height of the equivalent sand roughness k = 1.25r was used in the computation [12]. It follows from the data in [5, 19] that R = −3.5 for a gradient-free flow, and R = −4.1 in the presence of a longitudinal pressure gradient for such a selection of the parameter k.

Represented in Fig. 4 is a comparison of a computation with the results of measuring θ (open circles) with c_f (dark points) in a gradient-free flow with u_e = 27.1 m/sec. Tests were performed for values j = 0, 0.002, and 0.004 (points 1-3, respectively) for the mass-transfer parameters.

A comparison with experimental data [19] obtained for an accelerating equilibrium flow (u_∞ = 26.4 m/sec, j = 0.0039) is presented in Fig. 5. The results of measuring the integral characteristics c_f, θ, δ^* (points 1-3, respectively) and their computed values (dashed curve is a computation of c_f with $\varkappa$ = 0.41) are compared in Fig. 5a. We note that good agreement between the value of $\varkappa$ computed from (3.1) and (3.2) and its experimental value is obtained in a computation for both the case presented here with (j = 0.0039, $\varkappa \approx 0.35$) and without blowing (j = 0, $\varkappa \approx 0.38$, the pressure gradient was the same as in the tests with blowing). A comparison with measurement data for the mean velocity u (points 4) and the turbulent shear stress $\langle u'v'\rangle$ (points 5) on the stream acceleration section (x = 1.07 m, u_e = 33.9 m/sec),

and also the mean velocity (points 6) on the gradient-free section (x = 1.47 m, u_e = 39.1 m/sec) is represented in Fig. 5b. It is seen that agreement is good for both the integral and the local parameters.

The author is grateful to E. G. Zaulichnii for attention to the research, and to O. A. Danilov for useful discussion.

LITERATURE CITED

1. F. A. Dvorak, "Calculation of turbulent boundary layers on rough surfaces in a pressure gradient," AIAA J., 7, No. 9 (1969).
2. G. F. Sivykh, "On a computation of friction and heat transfer on rough permeable planar and axisymmetric bodies," Izv. Akad. Nauk SSSR, Mekh. Zhidk. Gaza, No. 5 (1979).
3. G. L. Mellor and H. J. Herring, "A survey of the mean turbulent field closure models," AIAA J., 11, No. 5 (1973).
4. S. V. Patankar and D. B. Spalding, Heat and Mass Transfer in Boundary Layers; A General Calculation Procedure, Intertex, London (1970).
5. M. M. Pimenta, R. J. Moffat, and W. M. Kays, "The structure of a boundary layer on a rough wall with blowing and heat transfer," Trans. ASME J. Heat Transfer, 101, No. 2 (1979).
6. A. E. Perry and P. N. Joubert, "Rough-wall boundary layers in adverse pressure gradients," J. Fluid Mech., 17, Pt. 2 (1963).
7. E. R. Van Driest, "On turbulent flow near a wall," J. Aero. Sci., 23, No. 11 (1956).
8. T. Cebeci and K. C. Chang, "Calculation of incompressible rough-wall boundary-layer flows," AIAA J., 16, No. 7 (1978).
9. V. N. Pilipenko, "On the construction of turbulent viscosity in flow near a rough surface," Izv. Akad. Nauk SSSR, Mekh. Zhidk. Gaza, No. 2 (1976).
10. C. Economos, "A transformation theory for the compressible turbulent boundary layer with mass transfer," AIAA J., 8, No. 4 (1970).
11. R. B. Dean, "A single formula for the complete velocity profile in a turbulent boundary layer," Trans. ASME J. Basic. Eng., 98, No. 4 (1976).
12. H. Schlichting, Boundary Layer Theory, McGraw-Hill (1968).
13. G. B. Schubauer and K. M. Chen, "Turbulent flow," in: Turbulent Flow and Heat Transfer [Russian translation], IL, Moscow (1963).
14. R. A. McD. Galbraith and M. R. Head, "Eddy viscosity and mixing length from measured boundary-layer developments," Aeron. Q., 26, Pt. 2 (1975).
15. W. J. Glowacki and S. W. Chi, "Effect of pressure gradient on mixing length for equilibrium turbulent boundary layers," AIAA Paper No. 213 (1972).
16. W. J. Glowacki, "An improved mixing length formulation for turbulent boundary layers with free-stream pressure gradients," AIAA Paper No. 202 (1978).
17. R. L. Simpson, "Characteristics of turbulent boundary layers at low Reynolds numbers with and without transpiration," J. Fluid Mech., 42, No. 4 (1970).
18. R. L. Simpson, R. J. Moffat, and W. M. Kays, "The turbulent boundary layer on a porous plate; experimental skin friction with variable injection and suction," Int. J. Heat Mass Transfer, 12, No. 7 (1969).
19. H. W. Coleman, R. J. Moffat, and W. M. Kays, "The accelerated fully rough turbulent boundary layer," J. Fluid Mech., 82, Pt. 3 (1977).